



# An unusual case of necrobiotic xanthogranuloma with IgG- $\lambda$ monoclonal gammopathy presenting as cerebral manifestations

Yiman Li<sup>1#</sup>, Fengxi Chen<sup>1#</sup>, Jie Cheng<sup>1</sup>, Hongqin Liang<sup>1</sup>, Kang Chen<sup>1</sup>, Jing Li<sup>1</sup>, Jian Wang<sup>1</sup>, Ping Cai<sup>1</sup>, Jiang Zhu<sup>2</sup>, Hong Lu<sup>1</sup>, Xiaoming Li<sup>1</sup>

<sup>1</sup>Department of Radiology, Southwest Hospital, Army Medical University (Third Military Medical University), Chongqing, China; <sup>2</sup>Institute of Pathology and Southwest Cancer Center, Southwest Hospital, Third Military Medical University (Army Medical University), Chongqing, China

<sup>#</sup>These authors contributed equally to this work.

*Correspondence to:* Hong Lu; Xiaoming Li. Department of Radiology, Southwest Hospital, Army Medical University (Third Military Medical University), Gao Tan Yan Street, Shapingba District, Chongqing 400038, China. Email: 540731442@qq.com; 359261069@qq.com; Jiang Zhu. Institute of Pathology and Southwest Cancer Center, Southwest Hospital, Third Military Medical University (Army Medical University) Gao Tan Yan Street, Shapingba District, Chongqing 400038, China. Email: zj972206@163.com.

**Keywords:** Necrobiotic xanthogranuloma (NXG); immunoglobulin G- $\lambda$  (IgG- $\lambda$ ); cerebral; meninges; magnetic resonance imaging (MRI)

Submitted Jun 17, 2022. Accepted for publication Dec 20, 2022. Published online Feb 01, 2023.

doi: 10.21037/qims-22-622

View this article at: <https://dx.doi.org/10.21037/qims-22-622>

## Introduction

Necrobiotic xanthogranuloma (NXG) disease is a rare non-Langerhans cell tissue proliferative disease that was first reported in 1980 (1). It is often associated with the abnormal proliferation of monoclonal gammopathy (M) protein. Among all cases with NXG, 50% of are immunoglobulin G (IgG)- $\kappa$  type, the rarer IgG- $\lambda$  type accounts for about 21%, and the remaining 12% consists of IgA, IgG, polyclonal, and unspecified types, with 17% being without paraproteinemia (2). Studies have shown that paraproteins play an essential role in granulation tissue formation (3). The disease often occurs in women over 60 years old, and the female-to-male ratio is about 1.7:2.7 (2,4). Nelson *et al.* (2) proposed the diagnostic criteria of NXG based on primary and secondary clinical and histopathological findings. The primary conditions include (I) yellow or orange papulonodular plaques on the skin that are (II) consistent with histopathological features demonstrating palisading granulomas with lymphoplasmacytic infiltrate and zones of necrobiosis. The secondary conditions include (I) paraproteinemia, plasmacytoid disease, and/or other related lymphoproliferative disorders; and (II) distribution in the periorbital skin. After exclusion of a foreign body, infection,

or other determinable diseases, the diagnosis is established by meeting the primary conditions and at least 1 secondary condition. NXG most commonly involves the skin (5), NXG involvement of the nervous system is especially rare. Herein, we report a case of NXG of the meninges, brain parenchyma, and spleen. We also summarize its clinical characteristics, imaging manifestations, histopathology, and therapeutic methods.

## Case presentation

All procedures performed in this study were performed in accordance with the ethical standards of the institutional and/or national research committee(s) and with the Helsinki Declaration (as revised in 2013). Written informed consent was provided by the patient for publication of this case report and accompanying images. A copy of the written consent is available for review by the editorial office of this journal.

The patient was a 63-year-old male who had a yellowish mass over the forehead and orbit (*Figure 1A,1B*) for more than 10 years. The mass showed progressive enlargement over the forehead, and there were flat yellowish skin lesions over the left side of the neck and chest. He had a history of

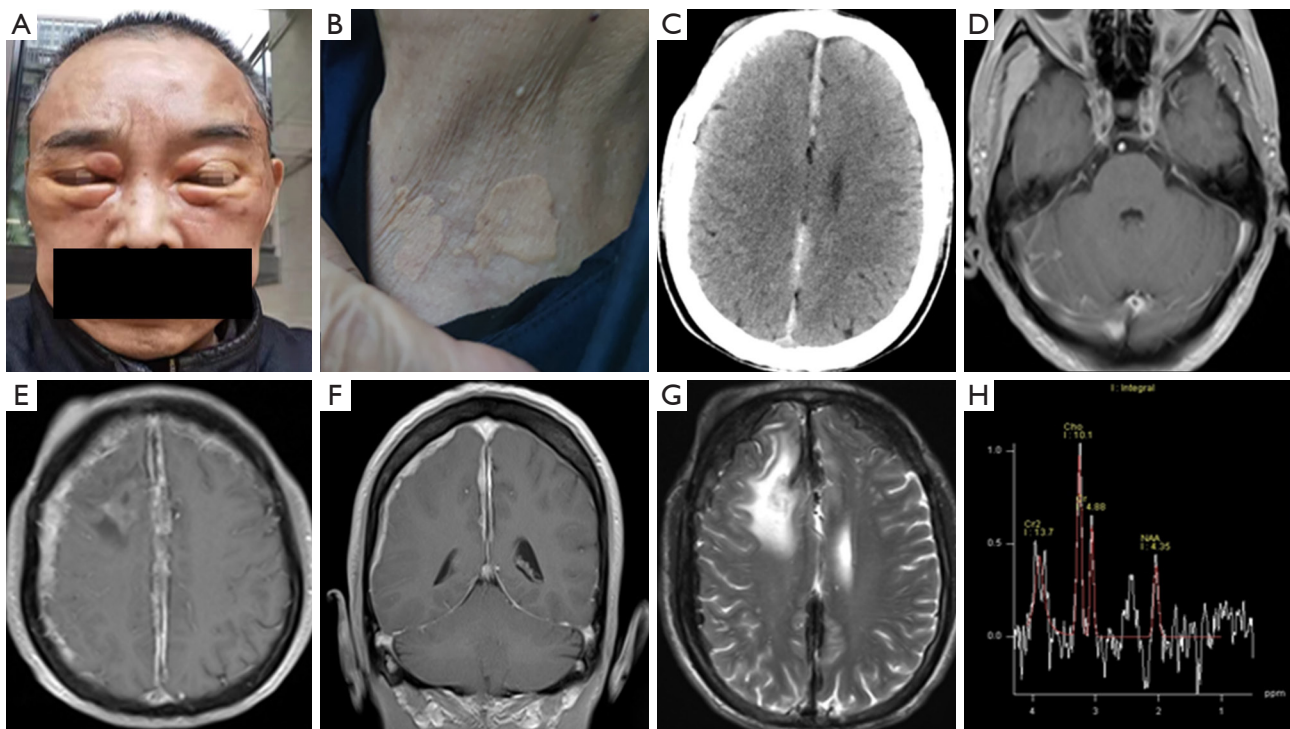


**Figure 1** The CT and MRI images of a 63-year-old male patient with NXG. The photograph of the patient (A) presenting with bilateral orbital pale-yellow masses, and (B) flat yellow skin lesions over the neck and chest. The plain CT (C) shows diffuse thickening and increased density of the meninges. MRI T2WI (D) shows a mass with high signal in the right frontal lobe with obvious surrounding edema. (E) The dynamic enhanced MRI. The right temporal muscle (E) is significantly enhanced, and the meninges (F) were extensively thickened and markedly heterogeneously enhanced. Coronal enhanced T1WI (F) shows that the tentorium cerebelli is not involved. MRS (G) shows that the peak of NAA is decreased and Cho is increased in the right frontal lobe lesions, Cho:NAA (H) >2. (This image was published with the patient's consent). CT, computed tomography; MRI, magnetic resonance imaging; NXG, necrobiotic xanthogranuloma; T2WI, T2-weighted imaging; T1WI, T1-weighted imaging; MRS, magnetic resonance spectroscopy; Cho, cholesterol; NAA, N-acetyl aspartate.

chronic liver disease and splenomegaly. He had undergone splenectomy 2 years prior due to progressive enlargement of splenic hemangioma and hypersplenism. He also experienced paroxysmal loss of consciousness and limb convulsions for 2 years, and was on oral levetiracetam tablets for antiepileptic treatment, with no current epilepsy symptoms. Laboratory biochemical tests revealed the following: an erythrocyte sedimentation rate (ESR) of 120 mm/h (normal range, 0–20 mm/h), a white blood cell count (WBC) of  $11.53 \times 10^9/L$  [normal range,  $(3.5-9.5) \times 10^9/L$ ], a high-sensitivity C-reactive protein (hsCRP) level of 84.6 (normal range, 0–7.44), a high-density lipoprotein cholesterol (HDL-C) level of 0.82 mmol/L (normal range, 0.9–2 mmol/L), an IgG ( $\lambda$ ) M-protein-positive status in serum protein electrophoresis, and an IgG level of 33.30 g/L (normal range, 7.82–16.8 g/L). The lambda light chain was 31.8 g/L (normal range, 3.13–7.23 g/L).

Cranial plain computed tomography (CT) scan

(Figure 1C) and enhanced magnetic resonance imaging (MRI) examination showed diffuse inhomogeneous thickening of the convex dura and cerebral falx. The enhanced scan showed inhomogeneous enhancement. After a further 10 months, the frontal mass had progressed, and a repeat enhanced MRI showed multiple soft tissue masses in the right frontal, orbital subcutaneous, and right temporal muscles. The enhanced scan showed significant enhancement of soft tissue masses (Figure 1D,1E). The diffuse and inhomogeneous thickening of the meninx was significantly aggravated compared with that of the previous examination. The lesion did not involve the tentorium cerebelli and showed an iso- and hypointensity on T1-weighted imaging (T1WI), and a mixed hyper- and hypointensity was observed on T2-weighted imaging (T2WI). Diffusion-weighted imaging (DWI) showed isointensity and obvious uneven enhancement (Figure 1F).

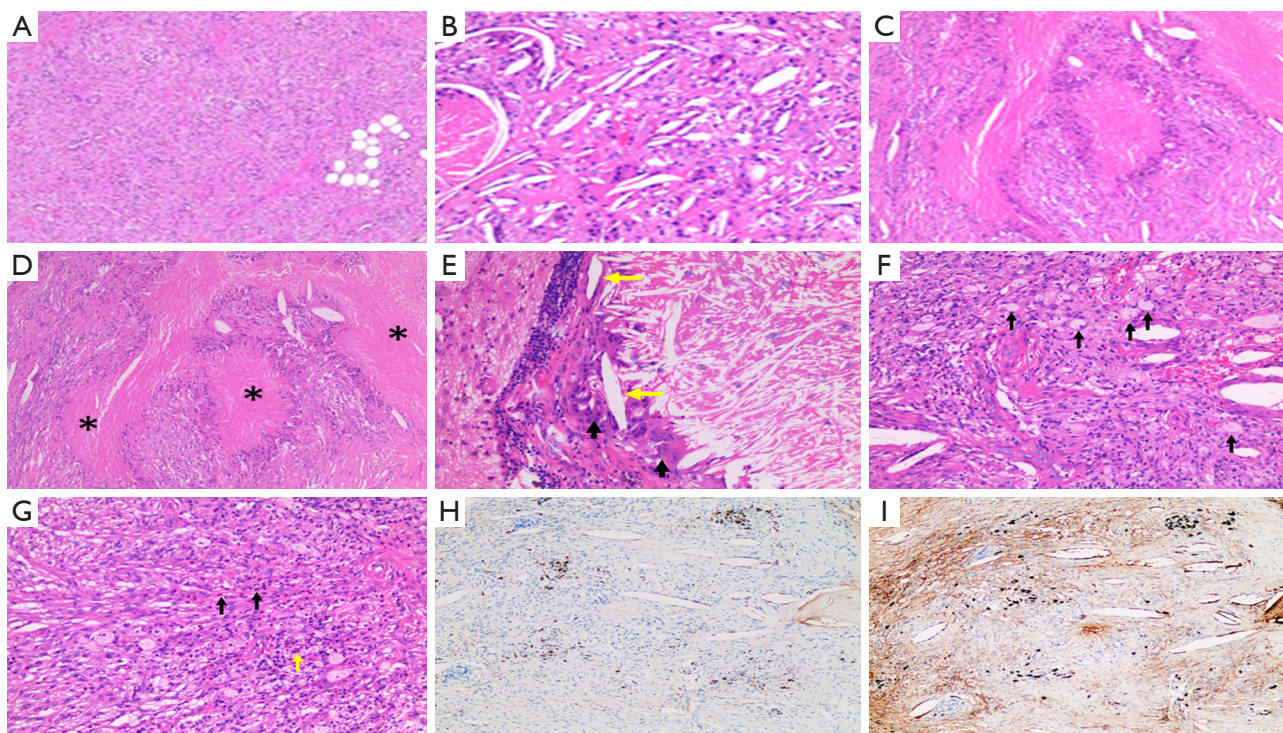


**Figure 2** Pathology of the right frontal subcutaneous mass (A) showing multifocal histiocytic infiltration (HE,  $\times 100$ ). Right frontal lobe pathology (B) showing foam cell infiltration and deposition of cholesterol crystals with focal necrosis (HE,  $\times 200$ ). The meningeal biopsy (C) and the necrotic lesions (D) showing a banded arrangement of granulomatous lesions with progressive foci of necrosis visible (\*) (HE,  $\times 200$ ). (E) Pathological tests showing multinucleated giant cells (black arrows) and cholesterol crystals (yellow arrows) around the necrotic foci (HE,  $\times 400$ ). (F) Pathological tests showing foam cells with nodular proliferation (black arrows) (HE,  $\times 400$ ). (G) Pathological tests showing infiltrating lymphocytes, plasma cells (yellow arrow), and eosinophils (black arrows) (HE,  $\times 400$ ). (H,I) Immunohistochemical staining for kappa light chains (H,  $\times 200$ ) and lambda light chains (I,  $\times 200$ ) showing polyclonal plasma cells infiltration. HE, hematoxylin and eosin.

The diameter of the mass on the right frontal lobe was about 2.8 cm (Figure 1G), with hypointensity on T1WI and hyperintensity on T2WI. The enhanced scan showed mild uneven enhancement, and large patchy edema was observed around the lesion. Magnetic resonance spectroscopy (MRS) showed decreased N-acetyl aspartate (NAA) peak, increased cholesterol (Cho) peak, and a Cho:NAA ratio  $>2$  (Figure 1H). The bone scan was normal.

Resections of the right frontal subcutaneous mass and frontal lobe lesion were carried out, and a biopsy of the meninx was also performed. During the operation, extensive pale yellow and tough lesions were found below the dura. The pathological properties of the lesions in the frontal scalp (Figure 2A), frontal lobes (Figure 2B), and meninges (Figure 2C) were consistent, showing significant histiocyte infiltration with fibrous tissue hyperplasia, as well as multifocal necrosis and degeneration. The pathological specimens showed the necrotic lesions (Figure 2D),

multinucleated giant cells, Cho crystals (Figure 2E), and foam cells (Figure 2F), with infiltrating lymphocytes, plasma cells, and eosinophils (Figure 2G). The immunohistochemical (IHC) staining of Kappa light chain (Figure 2H) showed weak positive for polyclonal plasma cell infiltration. The lambda light chain (Figure 2I) IHC staining showed polyclonal plasma cell infiltration. Other IHC staining revealed the following: S100 (-), CD68 (+), CD34 (+), and CD1a (-). Polymerase chain reaction (PCR) analysis showed no *BRAF V600E* mutation, and no *BRAF K-RAS*, *N-RAS*, or *PIK3CA* mutations were detected. Considering the finding of positive IgG ( $\lambda$ ) M-protein status before surgery, we established the final diagnosis of NXG with abnormal proliferation of IgG ( $\lambda$ ) M-protein. Due to poor compliance, the patient was not treated after the operation. Half a year later, the follow-up imaging showed no progress. The patient underwent bone marrow puncture and was started on oral cyclophosphamide and lenalidomide chemotherapy.

## Discussion

According to the latest revised classification (6), NXG belongs to the group C Langerhans cell proliferative diseases and has an unclear pathogenesis. Some researchers speculate that the disease may be related to low levels of HDL-C and M protein interaction disrupting the lipid homeostasis of macrophages, promoting inflammatory factor release, and producing immune complexes (7). NXG is related to abnormal proliferation of M protein (8-10), and the median time for multiple myeloma evolution is 5.7 years (2), requiring long-term monitoring of M protein levels (2,11). The clinical signs often affect the periorbital skin, with light yellow or orange pimple-like lesions. Multiple organs may be involved, such as the gastrointestinal tract, heart, liver, spleen, lung, and bone (5,12). Involvement of the nervous system is very rare, and was only reported in 2004 by Shah *et al.*, who described a case of bilateral frontal lobe parenchymal NXG but not involving the meninges or frontal scalp (13). The pathological features of their case included foam cell infiltration, focal necrosis, surrounding Touton giant cells, and Cho crystals. Representative IHC markers included CD68 (+), MAC387 (+), S100 (-), and CD1a (-) (14), which were consistent with the results of this case. The disease needs to be differentiated from xanthelasma, lipid necrosis, foreign body granuloma, and other non-Langerhans histiocytic hyperplasia such as Erdheim-Chester disease (15).

The imaging findings of brain involvement of NXG with abnormal IgG- $\lambda$  type M protein proliferation have not been reported. In the frontal region, the signal was slightly lower on T1WI and slightly higher on T2WI, and the scan showed obvious enhancement, which may be related to small vessel hyperplasia in the lesion. The head CT scan mainly showed diffuse uneven thickening of the meninges with high-density shadow, which was consistent with the case report of Shah *et al.* (13). The thickened meninges had rough and uneven edges. T1WI showed a high-low mixed signal, which might have resulted from the reduction of T1 relaxation time due to the large amount of Cho in the lesion (16). In contrast, the low signal might have been related to the presence of necrotic components and fibrous tissue hyperplasia with obvious uneven enhancement. The lesions in the right frontal lobe presented low signal intensity on T1WI and slightly high signal intensity on T2WI, and large patchy edema was observed around the lesion. MRS showed a Cho to NAA ratio  $>2$ , which was similar to that in glioma. Due to the histopathological

manifestations of neuronal damage and abnormal proliferation of glioma, pathologists initially misdiagnosed it as glioma before surgery. The imaging findings of NXG in the brain parenchyma were nonspecific and were easily misdiagnosed as a common craniocerebral malignant tumor before surgery. Compared with the scalp and frontal lobe lesions, the meningeal lesions were more extensive. However, the meningeal thickening in this patient did not involve the cerebellar tentorium, the thickened meningeal edges were not smooth, and the density and signal were obviously uneven. This is easily distinguishable from other diseases that cause diffuse meningeal thickening such as tuberculous meningitis, idiopathic hypertrophic meningitis, postoperative reactive thickening, hypocranial pressure syndrome, and lymphoma, but requires a detailed clinical history and laboratory biochemical examination. Due to the lack of relevant literature reports, further research is required to confirm the characteristic manifestations of the disease, which could include uneven thickening of the meningeal margins, uneven density and signal, and sparing of the tentorium.

In addition, the patient had concomitant splenic hemangioma, splenomegaly, and hypersplenism 10 years prior, as well as chronic liver disease without cirrhosis. Due to the enlarged size of splenic hemangioma, the possibility of malignant disease could not be completely ruled out before surgery, so splenectomy was performed. Dellatorre *et al.* (15) also found concurrent splenomegaly in an NXG patient, but the cause was unknown. Unfortunately, a pathological biopsy had not been performed. The retrospective pathological analysis found large patchy necrosis and the formation of peripheral granulation tissue. After excluding the causes of liver cirrhosis and heart disease, we speculated that splenomegaly and splenic hemangioma enlargement might be related to NXG.

There is no standard for the treatment of NXG. A systematic review by Steinhelfer *et al.* (17) concluded that many treatments are used for NXG, including intravenous immunoglobulin (IVIG), systemic corticosteroids, immunotherapy, antimetabolites, and tumor necrosis factor (TNF) inhibitors, but the first-line treatment should be recommended as corticosteroids and/or IVIG. The patient was not treated after the operation. Half a year later, the MRI examination of diffuse meningeal lesions showed no progress, and the spinal vertebrae did not show the typical manifestations of myeloma. Due to the absence of clear-cut guidelines of how to treat this rare disorder, a previous study (18) suggested that paraprotein should be the target of

therapeutic strategies. In this case, cyclophosphamide and lenalidomide were attempted for chemotherapy to prevent the progression of multiple myeloma. As of the time of writing, the patient is generally in good condition, and his follow-up is ongoing.

## Conclusions

NXG with IgG- $\lambda$  type abnormal proliferation is very rare and involves multiple systems, requiring a multidisciplinary diagnosis. In patients exhibiting multiple dermatological xanomatoid lesions involving the nervous system and abnormal imaging manifestations of meninges and brain parenchyma, the possibility of NXG should be considered after the exclusion of other diseases. Surgical resection or needle biopsy should be performed to confirm the diagnosis.

## Acknowledgments

*Funding:* This study was supported by the National Key Research and Development Program of China (No. 2016YFC0107101 to JW).

## Footnote

*Conflicts of Interest:* All authors have completed the ICMJE uniform disclosure form (available at <https://qims.amegroups.com/article/view/10.21037/qims-22-622/coif>). JW report that this study was supported by the National Key Research and Development Program of China (No. 2016YFC0107101). The authors have no other conflicts of interest to declare.

*Ethical Statement:* The authors are accountable for all aspects of the work in ensuring that questions related to the accuracy or integrity of any part of the work are appropriately investigated and resolved. All procedures performed in this study were in accordance with the ethical standards of the institutional and/or national research committee(s) and with the Helsinki Declaration (as revised in 2013). Written informed consent was provided by the patient for publication of this case report and accompanying images. A copy of the written consent is available for review by the editorial office of this journal.

*Open Access Statement:* This is an Open Access article distributed in accordance with the Creative Commons

Attribution-NonCommercial-NoDerivs 4.0 International License (CC BY-NC-ND 4.0), which permits the non-commercial replication and distribution of the article with the strict proviso that no changes or edits are made and the original work is properly cited (including links to both the formal publication through the relevant DOI and the license). See: <https://creativecommons.org/licenses/by-nc-nd/4.0/>.

## References

1. Kossard S, Winkelmann RK. Necrobiotic xanthogranuloma with paraproteinemia. *J Am Acad Dermatol* 1980;3:257-70.
2. Nelson CA, Zhong CS, Hashemi DA, Ashchyan HJ, Brown-Joel Z, Noe MH, Imadojemu S, Micheletti RG, Vleugels RA, Wanat KA, Rosenbach M, Mostaghimi A. A Multicenter Cross-Sectional Study and Systematic Review of Necrobiotic Xanthogranuloma With Proposed Diagnostic Criteria. *JAMA Dermatol* 2020;156:270-9.
3. Dholaria BR, Cappel M, Roy V. Necrobiotic xanthogranuloma associated with monoclonal gammopathy: successful treatment with lenalidomide and dexamethasone. *Ann Hematol* 2016;95:671-2.
4. Szalat R, Arnulf B, Karlin L, Rybojad M, Asli B, Malphettes M, Galicier L, Vignon-Pennamen MD, Harel S, Cordoliani F, Fuzibet JG, Oksenhendler E, Clauvel JP, Brouet JC, Feraud JP. Pathogenesis and treatment of xanthomatosis associated with monoclonal gammopathy. *Blood* 2011;118:3777-84.
5. Hilal T, DiCaudo DJ, Connolly SM, Reeder CB. Necrobiotic xanthogranuloma: a 30-year single-center experience. *Ann Hematol* 2018;97:1471-9.
6. Emile JF, Abla O, Fraitag S, Horne A, Haroche J, Donadieu J, et al. Revised classification of histiocytoses and neoplasms of the macrophage-dendritic cell lineages. *Blood* 2016;127:2672-81.
7. Szalat R, Pirault J, Feraud JP, Carrié A, Saint-Charles F, Olivier M, Robillard P, Frisdal E, Villard EF, Cathébras P, Bruckert E, Chapman MJ, Giral P, Guerin M, Lesnik P, Le Goff W. Physiopathology of necrobiotic xanthogranuloma with monoclonal gammopathy. *J Intern Med* 2014;276:269-84.
8. Wood AJ, Wagner MV, Abbott JJ, Gibson LE. Necrobiotic xanthogranuloma: a review of 17 cases with emphasis on clinical and pathologic correlation. *Arch Dermatol* 2009;145:279-84.
9. Sanz-Marco E, España E, López-Prats MJ, Chirivella-Casanova M, Aviño J, Díaz-Llopis M. Necrobiotic

- xanthogranuloma. Differential diagnosis, treatment and systemic involvement. Case report. *Arch Soc Esp Oftalmol* 2014;89:186-9.
10. Kim JG, Kim HR, You MH, Shin DH, Choi JS, Bae YK. Necrobiotic Xanthogranuloma Coexists with Diffuse Normolipidemic Plane Xanthoma and Multiple Myeloma. *Ann Dermatol* 2020;32:53-6.
  11. Higgins LS, Go RS, Dingli D, Kumar SK, Rajkumar SV, Dispenzieri A, Buadi FK, Lacy MQ, Lust JA, Kapoor P, Leung N, Lin Y, Kourelis TV, Gertz MA, Kyle RA, Gonsalves WI. Clinical Features and Treatment Outcomes of Patients With Necrobiotic Xanthogranuloma Associated With Monoclonal Gammopathies. *Clin Lymphoma Myeloma Leuk* 2016;16:447-52.
  12. Santosaputri E, Ellis EJ, Nagiah S, Chrispal A, Thomas A. A multisystem granulomatous disease: necrobiotic xanthogranuloma with hepatic involvement. *Med J Aust* 2014;200:490-3.
  13. Shah KC, Poonnoose SI, George R, Jacob M, Rajshekhar V. Necrobiotic xanthogranuloma with cutaneous and cerebral manifestations. Case report and review of the literature. *J Neurosurg* 2004;100:1111-4.
  14. Balagula Y, Straus DJ, Pulitzer MP, Lacouture ME. Necrobiotic xanthogranuloma associated with immunoglobulin m paraproteinemia in a patient with Waldenström macroglobulinemia. *J Clin Oncol* 2011;29:e305-7.
  15. Dellatorre G, Miqueloto JK. Necrobiotic Xanthogranuloma. *JAMA Dermatol* 2020;156:696.
  16. Ginat DT, Meyers SP. Intracranial lesions with high signal intensity on T1-weighted MR images: differential diagnosis. *Radiographics* 2012;32:499-516.
  17. Steinhelfer L, Kühnel T, Jäggle H, Mayer S, Karrer S, Haubner F, Schreml S. Systemic therapy of necrobiotic xanthogranuloma: a systematic review. *Orphanet J Rare Dis* 2022;17:132.
  18. Khan IJ, Azam NA, Sullivan SC, Habboush HW, Christian A. Necrobiotic xanthogranuloma successfully treated with a combination of dexamethasone and oral cyclophosphamide. *Can J Ophthalmol* 2009;44:335-6.

**Cite this article as:** Li Y, Chen F, Cheng J, Liang H, Chen K, Li J, Wang J, Cai P, Zhu J, Lu H, Li X. An unusual case of necrobiotic xanthogranuloma with IgG- $\lambda$  monoclonal gammopathy presenting as cerebral manifestations. *Quant Imaging Med Surg* 2023;13(3):1983-1988. doi: 10.21037/qims-22-622